Ultrahigh electron acceleration and Compton emission spectra in a superintense laser pulse and a uniform axial magnetic field

Article *in* Physical review A, Atomic, molecular, and optical physics · March 2000

DOI: 10.1103/PhysRevA.61.043801

2 authors:

Yousef I Salamin
American University of Sharjah
103 PUBLICATIONS **2,554** CITATIONS

SEE PROFILE

Farhad H. M. Faisal
Bielefeld University
236 PUBLICATIONS **6,910** CITATIONS

SEE PROFILE

Ultrahigh electron acceleration and Compton emission spectra in a superintense laser pulse and a uniform axial magnetic field

Yousef I. Salamin*
Physics Department, Birzeit University, P.O. Box 14, Birzeit, West Bank, Palestine

F. H. M. Faisal†
Fakultät für Physik, Universität Bielefeld, 33615 Bielefeld, Germany
(Received 24 August 1999; published 1 March 2000)

Exact expressions for the electron trajectory and energy are discussed, which predict very high acceleration, in vacuum, by a laser field and a uniform magnetic field. The laser field is modeled by a $\sin^2$ pulse and the initial electron motion, propagation of the laser pulse, and the magnetic field are all chosen in the same direction. An acceleration gradient in the TeV/m range within a very short travel distance of the electron is shown to be possible when a resonance condition is initially met. The acceleration and radiation properties are investigated using a recent analytic solution [F. H. M. Faisal and Y. I. Salamin, Phys. Rev. A **60**, 2505 (1999)] of the corresponding relativistic equations of motion in the laboratory frame. The radiation losses are shown to remain small under the resonance condition and the associated weak emission spectra are found to be characterized by highly irregular line distributions.

PACS number(s): 42.65.−k, 52.40.Nk, 42.50.Vk, 52.75.Di

I. INTRODUCTION

To accelerate particles in vacuum to extremely high energies requires building huge conventional accelerators, a task becoming prohibitively costly. Thus the search for a novel mechanism of acceleration that would cut both size and cost seems inevitable. Attention has recently been turned toward employing intense laser pulses and other electromagnetic fields for guiding and accelerating charged particles [1–4]. Examples include the inverse Cherenkov accelerators [5], inverse free electron laser accelerators [6], and plasma laser accelerators [7,8]. Electron energy gradients of up to 50 GeV/m have recently been reached in self-modulated plasma-wakefield laser accelerators [9–12].

In order to reach an electron energy gradient in the range of several TeV/m, very high intensity laser fields must be employed. Recently [13,14] a scheme based on the interaction with an ultrashort superintense laser pulse has been suggested. The idea further depends, for achieving the desired energy gradient, on interaction with only a fraction of a laser pulse, provided the electron may be extracted from the interaction region at the right time.

The aim of the present paper is to report on a theoretical investigation of the scheme of achieving high particle acceleration in vacuum by an intense laser pulse propagating along the direction of a uniform magnetic field, with the particle, an electron for definiteness, injected initially in that same direction. Such an electron absorbs a lot of energy from the radiation field, provided some specialized condition is initially met. This effect was discussed for the first time many years ago by Roberts and Buchsbaum [15]. It has also been studied more recently by several authors [16–18] as the basis of a possible scheme to accelerate charged particles. Within this context it is understood that the role of the magnetic field is both to help guide the electron motion and to influence the laser field in a sensitive way, thus allowing for resonance energy absorption by the charged particle from the radiation field and, hence, causing it to accelerate tremendously within a short time.

Previous analytic discussions [16–18] have tackled the idealized constant amplitude plane-wave laser field case, and only indirectly. We will investigate the dynamics and the radiation emitted by the electron in a short *pulsed* laser field in the presence of a uniform axial magnetic field, analytically and numerically. To be specific, the analytic work will employ the phase of a $\sin^2$ envelope laser pulse as a variable in terms of which explicit expressions for the electron energy in the presence of both fields will be reported.

Let B_s denote the strength of the uniform magnetic field, c the speed of light in vacuum, m and e the mass and charge of the electron, and β_0 the forward initial speed of the electron scaled by the speed of light. It turns out that when the initial conditions and the laser field parameters are such as to make the ratio

$$r=\frac{eB_s}{mc\omega_l}\sqrt{\frac{1+\beta_0}{1-\beta_0}}=\frac{\omega_c}{\omega_l}\sqrt{\frac{1+\beta_0}{1-\beta_0}} \tag{1}$$

close to unity, subsequent motion of the electron changes quite dramatically as it absorbs a tremendous amount of energy from the radiation field. Note that r is nothing but the cyclotron frequency of the electron $\omega_c=eB_s/mc$ scaled by the Doppler-shifted frequency of the laser. Hence, $r=1$ corresponds to a resonance between the cyclotron frequency of the electron and the Doppler-shifted laser frequency.

The plan of the rest of the paper is as follows. We discuss first in Sec. II the electron trajectories when the abovementioned resonance condition is initially met. We will show that the parametric equations of the electron trajectory possess finite limits and may be written compactly as $r\to 1$. In Sec. III we report and discuss the exact expression for the electron energy under the same condition. It will be shown

*Electronic address: ysalamin@science.birzeit.edu
†Electronic address: ffaisal@physik.uni-bielefeld.de

that energy gradients of about several GeV/m may be achieved when the parameters are adjusted in such a way as to meet the resonance condition initially. More significantly, energy gradients in the TeV/m range will be shown to result from interaction of the electron with a fraction of a field cycle of an ultraintense pulse. Sections IV and V will be devoted to a study of the emission of radiation that accompanies the electron motion under these conditions. In Sec. IV, we will discuss the radiation losses in general and show that they are small in the present situation. We will finally give explicit illustrations of the emission spectra in different observation directions in Sec. V. Our conclusions will be given in Sec. VI.

II. THE ELECTRON TRAJECTORY EQUATIONS

Working fully relativistically (and employing a vector potential description for the radiation and the added uniform magnetic fields) we have recently obtained exact analytical trajectories for an electron in the simultaneous presence of a uniform magnetic field and an elliptically polarized constant amplitude plane-wave laser field [19]. More recently, analytic expressions of the electron trajectory have been derived [20] for an electron in a linearly-polarized $\sin^2$ laser *pulse* and an axial dc magnetic field. Letting A_l and B_s stand for the laser field peak intensity and uniform magnetic field strength, respectively, the associated field vectors were obtained from the potential

$$\mathbf{A}(\eta)=\hat{\mathbf{i}}A_l \sin^2\left(\frac{\kappa}{2}\eta\right)\cos\eta-\frac{B_s}{2}(\hat{\mathbf{i}}y-\hat{\mathbf{j}}x), \tag{2}$$

where κ is a real constant between zero and one. Note that κ is related to the pulse duration or full width at half maximum (FWHM), τ, by $\kappa=\pi/\omega\tau$ and to the number N of field cycles in the pulse by $N=1/\kappa$. Moreover, $\eta=\omega_l t-\mathbf{k}\cdot\mathbf{r}$, with $\mathbf{k}$ the wave vector whose magnitude is $k=\omega_l/c$, and t and $\mathbf{r}=(x,y,z)$ the time and space coordinates of the electron. Furthermore, the dimensionless laser intensity parameter $q=eA_l/mc^2$ will be used below, with $q^2=1$ being equivalent to the field intensity $\approx 10^{18}\,\mathrm{W/cm^2}$. With these notations, the trajectory of the electron in the presence of the vector potential (2) has been given explicitly [20] as

$$x(\eta)=\left(\frac{qc}{4\omega_l}\right)\gamma_0(1+\beta_0)\left\{\left[\frac{2}{1-r^2}\right]\sin\eta-\left[\frac{\kappa+1}{(\kappa+1)^2-r^2}\right]\sin[(\kappa+1)\eta]-\left[\frac{\kappa-1}{(\kappa-1)^2-r^2}\right]\sin[(\kappa-1)\eta]\right.$$
$$\left.+r\left[-\frac{2}{1-r^2}+\frac{1}{(\kappa+1)^2-r^2}+\frac{1}{(\kappa-1)^2-r^2}\right]\sin(r\eta)\right\}, \tag{3}$$

$$y(\eta)=-\left(\frac{qc}{4\omega_l}\right)\gamma_0(1+\beta_0)r\left\{\left[\frac{2}{1-r^2}\right]\cos\eta-\frac{\cos[(\kappa+1)\eta]}{(\kappa+1)^2-r^2}-\frac{\cos[(\kappa-1)\eta]}{(\kappa-1)^2-r^2}\right.$$
$$\left.+\left[-\frac{2}{1-r^2}+\frac{1}{(\kappa+1)^2-r^2}+\frac{1}{(\kappa-1)^2-r^2}\right]\cos(r\eta)\right\}, \tag{4}$$

$$z(\eta)=\frac{c}{\omega_l}\left(\frac{\beta_0}{1-\beta_0}\right)\eta+\frac{c}{\omega_l}\frac{q^2}{16}\left(\frac{1+\beta_0}{1-\beta_0}\right)\left(\left[\frac{2}{1-r^2}\right]\left\{\left(\frac{\kappa+1}{2}\right)\left[\frac{(\kappa+2)\eta-\sin[(\kappa+2)\eta]}{(\kappa+2)^2}+\frac{\kappa\eta-\sin(\kappa\eta)}{\kappa^2}\right]+\left(\frac{\kappa-1}{2}\right)\right.\right.$$
$$\left.\times\left[\frac{\kappa\eta-\sin(\kappa\eta)}{\kappa^2}+\frac{(\kappa-2)\eta-\sin[(\kappa-2)\eta]}{(\kappa-2)^2}\right]-\left[\frac{2\eta-\sin(2\eta)}{4}\right]\right\}-\left[\frac{(\kappa+1)^2}{(\kappa+1)^2-r^2}\right]\left\{\left(\frac{\kappa+1}{2}\right)\right.$$
$$\times\left[\frac{2(\kappa+1)\eta-\sin[2(\kappa+1)\eta]}{4(\kappa+1)^2}\right]+\left(\frac{\kappa-1}{2}\right)\left[\frac{2\kappa\eta-\sin(2\kappa\eta)}{(2\kappa)^2}-\frac{2\eta-\sin(2\eta)}{4}\right]-\left[\frac{(\kappa+2)\eta-\sin[(\kappa+2)\eta]}{(\kappa+2)^2}\right.$$
$$\left.\left.-\frac{\kappa\eta-\sin(\kappa\eta)}{\kappa^2}\right]\right\}-\left[\frac{(\kappa-1)^2}{(\kappa-1)^2-r^2}\right]\left\{\left(\frac{\kappa+1}{2}\right)\left[\frac{2\kappa\eta-\sin(2\kappa\eta)}{(2\kappa)^2}+\frac{2\eta-\sin(2\eta)}{4}\right]+\left(\frac{\kappa-1}{2}\right)\right.$$
$$\left.\left.\times\left[\frac{2(\kappa-1)\eta-\sin[2(\kappa-1)\eta]}{4(\kappa-1)^2}\right]-\left[\frac{\kappa\eta-\sin(\kappa\eta)}{\kappa^2}-\frac{(\kappa-2)\eta-\sin[(\kappa-2)\eta]}{(\kappa-2)^2}\right]\right\}+r^2\left[-\frac{2}{1-r^2}+\frac{1}{(\kappa+1)^2-r^2}\right.\right.$$
$$\left.\left.+\frac{1}{(\kappa-1)^2-r^2}\right]\left\{\left(\frac{\kappa+1}{2}\right)\left[\frac{(\kappa+1+r)\eta-\sin[(\kappa+1+r)\eta]}{(\kappa+1+r)^2}+\frac{(\kappa+1-r)\eta-\sin[(\kappa+1-r)\eta]}{(\kappa+1-r)^2}\right]\right.\right.$$

$$+\left(\frac{\kappa-1}{2}\right)\left[\frac{(\kappa-1+r)\eta-\sin[(\kappa-1+r)\eta]}{(\kappa-1+r)^2}+\frac{(\kappa-1-r)\eta-\sin[(\kappa-1-r)\eta]}{(\kappa-1-r)^2}\right.$$
$$\left.-\left[\frac{(1+r)\eta-\sin[(1+r)\eta]}{(1+r)^2}+\frac{(1-r)\eta-\sin[(1-r)\eta]}{(1-r)^2}\right]\right\}\Bigg). \tag{5}$$

In Fig. 1 we show a three-dimensional (3D) *off-resonance* trajectory for an electron moving initially along $+z$ at the scaled speed $\beta_0\approx 0.994987$ ($\gamma_0=10$). For the set of parameters employed $r\approx 0.044612$ and thus the system is far from being in resonance. In this situation, the electron spirals out of and around its initial direction of motion, with the amplitude of its transverse motion reaching a maximum when it encounters the peak pulse intensity. Then it is seen to spiral in and toward its initial direction of travel and finally it is left behind the trailing edge of the pulse. As a result, hardly any energy absorbed by the electron in the course of its interaction with the field is retained at the end of the pulse.

But, close to resonance, say $r=1.001$, we get the 3D trajectory shown in Fig. 2. Figure 2 has been produced employing Eqs. (3)–(5) after γ_0 and β_0 have been eliminated from them in favor of $r\approx 1.001$ using Eq. (1). The remaining parameters have the same values as in Fig. 1. Here, although the condition for resonance is only approximately met, the electron in fact absorbs a tremendous net amount of energy from the pulse. This may be inferred from the fact that it spirals outward and advances forward a much longer distance before it is left behind the pulse, retaining most, if not all, of the energy it has absorbed.

Under the condition of *exact resonance*, $r=1$, in the linearly polarized $\sin^2$ pulse, the trajectory equations take the form

$$x(\eta)\rightarrow\left(\frac{qc}{4\omega_c}\right)\left\{\eta\cos\eta-\left[\frac{\kappa+1}{\kappa(\kappa+2)}\right]\sin[(\kappa+1)\eta]-\left[\frac{\kappa-1}{\kappa(\kappa-2)}\right]\sin[(\kappa-1)\eta]+\left[\frac{\kappa^2-2}{\kappa^2-4}\right]\sin\eta\right\}, \tag{6}$$

$$y(\eta)\rightarrow\left(\frac{qc}{4\omega_c}\right)\left\{\eta\sin\eta+\frac{\cos[(\kappa+1)\eta]}{\kappa(\kappa+2)}+\frac{\cos[(\kappa-1)\eta]}{\kappa(\kappa-2)}-\left[\frac{2}{\kappa^2-4}\right]\cos\eta\right\}, \tag{7}$$

$$z(\eta)\rightarrow\frac{c}{\omega_l}\left(\left(\frac{\omega_l^2-\omega_c^2}{2\omega_c^2}\right)\eta+\frac{q^2}{96}\left(\frac{\omega_l}{\omega_c}\right)^2\eta^3+\frac{c}{\omega_l}\frac{q^2}{16}\left(\frac{\omega_l}{\omega_c}\right)^2\left(\frac{2}{\kappa^2-4}\right)\left\{\left(\frac{\kappa+1}{2}\right)\left[\frac{(\kappa+2)\eta-\sin[(\kappa+2)\eta]}{(\kappa+2)^2}+\frac{\kappa\eta-\sin(\kappa\eta)}{\kappa^2}\right]\right.$$
$$+\left(\frac{\kappa-1}{2}\right)\left[\frac{\kappa\eta-\sin(\kappa\eta)}{\kappa^2}+\frac{(\kappa-2)\eta-\sin[(\kappa-2)\eta]}{(\kappa-2)^2}\right]-\left[\frac{2\eta-\sin(2\eta)}{4}\right]\Bigg\}-\left[\frac{(\kappa+1)^2}{\kappa(\kappa+2)}\right]\Bigg\{\left(\frac{\kappa+1}{2}\right)$$
$$\times\left[\frac{2(\kappa+1)\eta-\sin[2(\kappa+1)\eta]}{4(\kappa+1)^2}\right]+\left(\frac{\kappa-1}{2}\right)\left[\frac{2\kappa\eta-\sin(2\kappa\eta)}{(2\kappa)^2}-\frac{2\eta-\sin(2\eta)}{4}\right]-\left[\frac{(\kappa+2)\eta-\sin[(\kappa+2)\eta]}{(\kappa+2)^2}\right.$$
$$\left.-\frac{\kappa\eta-\sin(\kappa\eta)}{\kappa^2}\right]\Bigg\}-\left[\frac{(\kappa-1)^2}{\kappa(\kappa-2)}\right]\Bigg\{\left(\frac{\kappa+1}{2}\right)\left[\frac{2\kappa\eta-\sin(2\kappa\eta)}{(2\kappa)^2}+\frac{2\eta-\sin(2\eta)}{4}\right]+\left(\frac{\kappa-1}{2}\right)$$
$$\times\left[\frac{2(\kappa-1)\eta-\sin[2(\kappa-1)\eta]}{4(\kappa-1)^2}\right]-\left[\frac{\kappa\eta-\sin(\kappa\eta)}{\kappa^2}-\frac{(\kappa-2)\eta-\sin[(\kappa-2)\eta]}{(\kappa-2)^2}\right]\Bigg\}+\left(\frac{\kappa+1}{2}\right)$$
$$\times\left\{\left[\frac{(\kappa+2)\eta-\sin[(\kappa+2)\eta]}{(\kappa+2)^2}\right]\left[\frac{2\kappa+2}{\kappa+2}\right]+\frac{\eta-\eta\cos[(\kappa+2)\eta]}{(\kappa+2)^2}+\left[\frac{\kappa\eta-\sin(\kappa\eta)}{\kappa^2}\right]\left[\frac{2\kappa+2}{\kappa}\right]-\frac{\eta-\eta\cos(\kappa\eta)}{\kappa^2}\right\}$$

$$+\left(\frac{\kappa-1}{2}\right)\left\{\left[\frac{\kappa\eta-\sin(\kappa\eta)}{\kappa^2}\right]\left[\frac{2\kappa-2}{\kappa}\right]+\frac{\eta-\eta\cos(\kappa\eta)}{\kappa^2}+\left[\frac{(\kappa-2)\eta-\sin[(\kappa-2)\eta]}{(\kappa-2)^2}\right]\left[\frac{2\kappa-2}{\kappa-2}\right]\right.$$
$$\left.-\frac{\eta-\eta\cos[(\kappa-2)\eta]}{(\kappa-2)^2}\right\}-\left[\frac{3\eta-\sin(2\eta)-\eta\cos(2\eta)}{4}\right]\Bigg). \tag{8}$$

In arriving at Eqs. (6)–(8), Eq. (1) has been used to eliminate γ_0 and β_0 in favor of ω_c and ω_l. Equations (6)–(8) were then used to produce a 3D trajectory corresponding to the same values of the remaining parameters as were used in Fig. 2. The exact resonance and near-resonance conditions led to virtually indistinguishable trajectories, all other parameters being identical. This forces upon us the conclusion that one may not need to meet the delicate balance of parameters required by the condition of exact resonance, but that meeting such a condition approximately is perhaps good enough to trigger the enhanced energy absorption by the electron from the radiation field.

To sum up, we have shown in this section that the highly symmetric trajectory of an electron in a laser plus uniform magnetic fields changes quite dramatically when the parameters conspire with the initial conditions to render the electron cyclotron frequency equal to the Doppler-shifted frequency of the laser. Recall that a linearly polarized wave may be viewed as a superposition of two (left- and right-circularly polarized) waves with half the total intensity each. As has been explained in the past [17], when the resonance condition is met, the electron moves in phase with the electric field associated with one of the circularly polarized halves of the wave. As a result the electron continues to be accelerated by this electric field. The correctness of our derived trajectory equations under the condition of exact resonance has also been demonstrated numerically. In the next section, we will show the dramatic change in the process of energy exchange between the electron and the radiation field that results when the conditions for near or exact resonance are initially met.

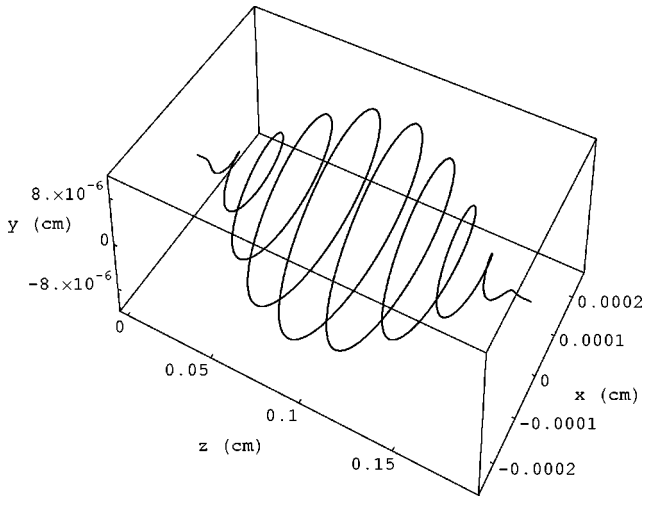

FIG. 1. Electron trajectory in a linearly polarized $\sin^2$ laser pulse of wavelength $\lambda=800$ nm and intensity corresponding to $q=1$, and a magnetic field of strength $B_s=30$ T, calculated for a pulse containing 10 field cycles ($\kappa=0.1$). The initial scaled electron energy is $\gamma_0=10$ ($E_0\approx4.5$ MeV), and hence $r\approx0.044612$, i.e., away from resonance.

III. THE ELECTRON ENERGY EQUATION

It has long been known [15] that an electron can gain tremendous energy through coherent interaction with an electromagnetic wave and a uniform magnetic field, provided (1) the wave vector **k** is parallel to the magnetic field $\mathbf{B}_s$; (2) the index of refraction of the medium in which propagation takes place $n\equiv kc/\omega_l=1$; and (3) the following condition is met:

$$\omega_l-\frac{\omega_c}{\gamma}-kv_z=0, \tag{9}$$

where v_z is the component of electron velocity parallel to $\mathbf{B}_s$ and γ is the Lorentz factor. It was shown many years ago by Roberts and Buchsbaum [15] that if the condition (9) is met initially, it will hold throughout the motion of the electron in the fields considered.

Note that at $t=0$ the condition (9) is exactly equivalent to our resonance condition $r=1$. Moreover, we have shown [19,20] that

$$\gamma(1-\beta_z)=\gamma_0(1-\beta_0). \tag{10}$$

This implies that if the resonance condition is met initially,

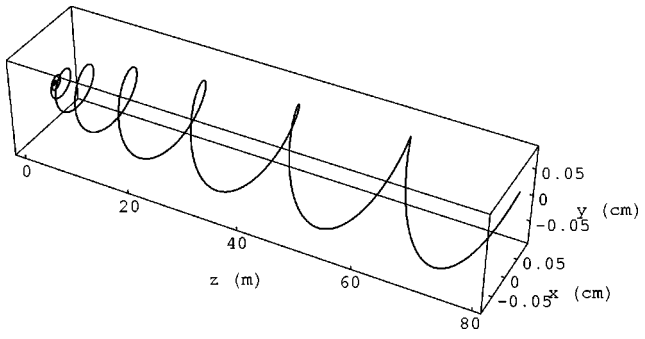

FIG. 2. Electron trajectory in a linearly polarized $\sin^2$ laser pulse of wavelength $\lambda=800$ nm and intensity corresponding to $q=1$, and a magnetic field of strength $B_s=30$ T, calculated for a pulse containing 10 field cycles ($\kappa=0.1$). The initial scaled electron energy γ_0 is such as to make $r=1.001$, i.e., near resonance.

then it will hold for all times, in agreement with Eq. (9). Furthermore, Eq. (10) is a statement of conservation of the quantity $\mathcal{E}/c-p_z$, where p_z is the z component of the momentum of the electron. From it one may also infer that the Doppler-shifted frequency of the laser field is a constant.

We now quote the associated expression for the electron energy derived recently [20], for the case of a linearly polarized laser pulse,

$$\gamma(\eta)=\gamma_0+\frac{q^2}{16}\gamma_0(1+\beta_0)\Bigg(\left[\frac{2}{1-r^2}\right]\left\{\left(\frac{\kappa+1}{2}\right)\left[\frac{1-\cos[(\kappa+2)\eta]}{\kappa+2}+\frac{1-\cos(\kappa\eta)}{\kappa}\right]+\left(\frac{\kappa-1}{2}\right)\left[\frac{1-\cos(\kappa\eta)}{\kappa}\right.\right.$$
$$\left.+\frac{1-\cos[(\kappa-2)\eta]}{\kappa-2}\right]-\left[\frac{1-\cos(2\eta)}{2}\right]\Bigg\}-\left[\frac{(\kappa+1)^2}{(\kappa+1)^2-r^2}\right]\Bigg\{\left(\frac{\kappa+1}{2}\right)\left[\frac{1-\cos[2(\kappa+1)\eta]}{2(\kappa+1)}\right]+\left(\frac{\kappa-1}{2}\right)\left[\frac{1-\cos(2\kappa\eta)}{2\kappa}\right.$$
$$\left.-\frac{1-\cos(2\eta)}{2}\right]-\left[\frac{1-\cos[(\kappa+2)\eta]}{\kappa+2}-\frac{1-\cos(\kappa\eta)}{\kappa}\right]\Bigg\}-\left[\frac{(\kappa-1)^2}{(\kappa-1)^2-r^2}\right]\Bigg\{\left(\frac{\kappa+1}{2}\right)\left[\frac{1-\cos(2\kappa\eta)}{2\kappa}+\frac{1-\cos(2\eta)}{2}\right]$$
$$+\left(\frac{\kappa-1}{2}\right)\left[\frac{1-\cos[2(\kappa-1)\eta]}{2(\kappa-1)}\right]-\left[\frac{1-\cos(\kappa\eta)}{\kappa}-\frac{1-\cos[(\kappa-2)\eta]}{\kappa-2}\right]\Bigg\}+r^2\Bigg[-\frac{2}{1-r^2}+\frac{1}{(\kappa+1)^2-r^2}$$
$$+\frac{1}{(\kappa-1)^2-r^2}\Bigg]\Bigg\{\left(\frac{\kappa+1}{2}\right)\left[\frac{1-\cos[(\kappa+1+r)\eta]}{\kappa+1+r}+\frac{1-\cos[(\kappa+1-r)\eta]}{\kappa+1-r}\right]+\left(\frac{\kappa-1}{2}\right)\left[\frac{1-\cos[(\kappa-1+r)\eta]}{\kappa-1+r}\right.$$
$$\left.\left.+\frac{1-\cos[(\kappa-1-r)\eta]}{\kappa-1-r}\right]-\left[\frac{1-\cos[(1+r)\eta]}{1+r}+\frac{1-\cos[(1-r)\eta]}{1-r}\right]\Bigg\}\Bigg). \tag{11}$$

The energy expression that holds when exact resonance is achieved may be obtained from Eq. (11) after some (rather lengthy) algebra. On exact resonance, the scaled electron energy becomes

$$\gamma(\eta)\to\frac{\omega_l^2+\omega_c^2}{2\omega_l\omega_c}\left\{1+\frac{q^2}{16}\left[\frac{\omega_l^2}{\omega_l^2+\omega_c^2}\right]\eta^2\right\}+\frac{q^2}{16}\left(\frac{\omega_l}{\omega_c}\right)\Bigg(\left[\frac{2}{\kappa^2-4}\right]\left\{\left(\frac{\kappa+1}{2}\right)\left[\frac{1-\cos[(\kappa+2)\eta]}{\kappa+2}+\frac{1-\cos(\kappa\eta)}{\kappa}\right]+\left(\frac{\kappa-1}{2}\right)\right.$$
$$\times\left.\left[\frac{1-\cos(\kappa\eta)}{\kappa}+\frac{1-\cos[(\kappa-2)\eta]}{\kappa-2}\right]-\left[\frac{1-\cos(2\eta)}{2}\right]\right\}-\left[\frac{(\kappa+1)^2}{\kappa(\kappa+2)}\right]\left\{\left(\frac{\kappa+1}{2}\right)\left[\frac{1-\cos[2(\kappa+1)\eta]}{2(\kappa+1)}\right]+\left(\frac{\kappa-1}{2}\right)\right.$$
$$\times\left.\left[\frac{1-\cos(2\kappa\eta)}{2\kappa}+\frac{1-\cos(2\eta)}{2}\right]-\left[\frac{1-\cos[(\kappa+2)\eta]}{\kappa+2}-\frac{1-\cos(\kappa\eta)}{\kappa}\right]\right\}-\left[\frac{(\kappa-1)^2}{\kappa(\kappa-2)}\right]\left\{\left(\frac{\kappa+1}{2}\right)\left[\frac{1-\cos(2\kappa\eta)}{2\kappa}\right.\right.$$
$$\left.+\frac{1-\cos(2\eta)}{2}\right]+\left(\frac{\kappa-1}{2}\right)\left[\frac{1-\cos[2(\kappa-1)\eta]}{2(\kappa-1)}\right]-\left[\frac{1-\cos(\kappa\eta)}{\kappa}-\frac{1-\cos[(\kappa-2)\eta]}{\kappa-2}\right]\Bigg\}+\left(\frac{\kappa+1}{2}\right)$$
$$\times\left\{\left[\frac{1-\cos[(\kappa+2)\eta]}{\kappa+2}\right]\left[\frac{2\kappa+3}{\kappa+2}\right]+\frac{\eta\sin[(\kappa+2)\eta]}{\kappa+2}+\left[\frac{1-\cos(\kappa\eta)}{\kappa}\right]\left[\frac{2\kappa+1}{\kappa}\right]-\frac{\eta\sin(\kappa\eta)}{\kappa}\right\}+\left(\frac{\kappa-1}{2}\right)\left\{\left[\frac{1-\cos(\kappa\eta)}{\kappa}\right]\right.$$
$$\times\left.\left[\frac{2\kappa-1}{\kappa}\right]+\frac{\eta\sin(\kappa\eta)}{\kappa}+\left[\frac{1-\cos[(\kappa-2)\eta]}{\kappa-2}\right]\left[\frac{2\kappa-3}{\kappa-2}\right]-\frac{\eta\sin[(\kappa-2)\eta]}{\kappa-2}\right\}-\left\{\left[\frac{1-\cos(2\eta)}{2}\right]\left[\frac{3}{2}\right]+\frac{\eta\sin(2\eta)}{2}\right\}\Bigg). \tag{12}$$

We show in Fig. 3 the energy vs the number of laser field cycles $\eta/2\pi$ (a,b), as well as vs the forward distance of travel during the interaction with the pulse (c,d), for exact resonance, $r=1$. The figure seems to suggest that, for a particular field intensity (q fixed), the maximum value attainable by γ is only limited by the number of field cycles in the pulse used. This is in sharp contrast with the nonresonance case we have discussed earlier [19,20] in which the electron essentially returns all the energy it gains back to the radiation field upon exit from the pulse envelope. Note, as well, the presence of small energy oscillations that arise from the trigonometric terms in Eq. (12). It is interesting to note that the energy gradient (roughly calculated here as the ratio of the net energy gain to the distance of travel in the forward direction during interaction) is about 0.38 GeV/m in Fig. 3(c). It would be, however, misleading to conclude, on the basis of

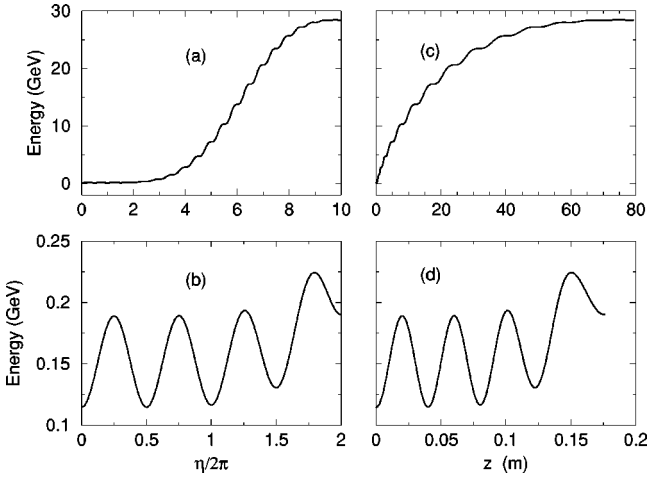

FIG. 3. Energy of the electron whose trajectory is given in Fig. 2. In (a) and (b) the energy is plotted vs the number of field cycles $\eta/2\pi$, while in (c) and (d) it is plotted vs the distance of travel along the z axis. Note that (b) and (d) have been produced by zooming on the portions of (a) and (c), respectively, that correspond to interaction with the first two field cycles.

Fig. 3 alone, that arbitrarily high energies can be obtained only by employing laser pulses of ever higher intensity and ever larger pulse duration. As Fig. 4 shows, interaction with such pulses takes place over correspondingly longer distances.

Closer scrutiny of the graphs of energy vs forward distance of travel, shown in Figs. 3 and 4, leads to a better understanding of the process of energy exchange between the electron and the radiation field. As the plots labeled (b) and (d) in both figures show, absorption of a huge amount of energy by the electron, per meter of travel, takes place during its encounter with the first *quarter* of a field cycle. In fact, according to Fig. 3(d) an energy gradient of 9.5 GeV/m is gained at $q=1$, while when zooming on the first quarter cycle of Fig. 4(d) (not shown) a gain of about 38 TeV/m is found at $q=100$, provided the electron can be extracted at the end of the first quarter cycle (e.g., among other possibilities, by matching the resonance over the distance corresponding only to one quarter period). Note that most of the energy gained in the first quarter cycle is deposited back into the radiation field during interaction with the second quarter cycle. However, it is also significant to note that more energy absorption and less reemission take place when the electron interacts with the successive quarter field cycles. Thus a net gain in energy builds up quickly and the electron advances forward a long distance.

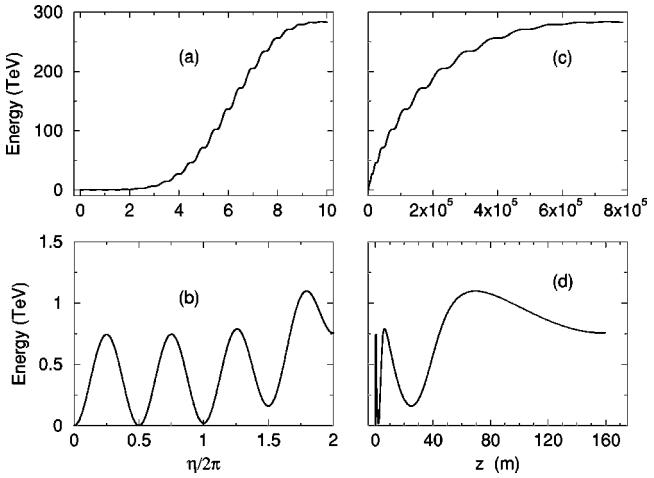

FIG. 4. Same as Fig. 3, but for $q=100$.

IV. RADIATION LOSS

We have been concerned thus far only with the acceleration of the electron. However, accelerated charged particles emit radiation and, therefore, can lose energy. Thus, radiation losses may place a limit on the maximum energy attainable by the particle in an accelerator. It is important, therefore, to investigate the radiation loss under the present scheme of acceleration. To this end we employ the relativistic generalization of the Larmor formula [21] for the total instantaneous power emitted by the electron,

$$P(t)=\frac{2}{3}\frac{e^2}{c}\gamma^6\left\{\left[\frac{d\boldsymbol{\beta}}{dt}\right]^2-\left[\boldsymbol{\beta}\times\frac{d\boldsymbol{\beta}}{dt}\right]^2\right\}, \tag{13}$$

where $\boldsymbol{\beta}$ is the instantaneous velocity of the electron scaled by the speed of light. We turn $P(t)$ into a function of the phase η using the chain rule of differentiation $d\boldsymbol{\beta}/dt=(d\boldsymbol{\beta}/d\eta)(d\eta/dt)$ and Eq. (10), together with a well-known vector identity. When the resonance condition is used to eliminate the dependence upon the initial velocity, there results

$$P(\eta)=\frac{2}{3}\frac{(e\omega_c\gamma)^2}{c}\left\{\left[\frac{d\boldsymbol{\beta}}{d\eta}\right]^2+\gamma^2\left[\boldsymbol{\beta}\cdot\frac{d\boldsymbol{\beta}}{d\eta}\right]^2\right\}. \tag{14}$$

A good qualitative measure of the energy loss may be obtained by considering the ratio of the power radiated to the energy gained within one cycle of the laser field. In other words, we define the ratio

$$\Gamma(\eta)=\frac{2\pi}{\omega_l}\frac{P}{\mathcal{E}}=\frac{4\pi}{3\omega_l c}\frac{(e\omega_c\gamma)^2}{\gamma mc^2}\left\{\left[\frac{d\boldsymbol{\beta}}{d\eta}\right]^2+\gamma^2\left[\boldsymbol{\beta}\cdot\frac{d\boldsymbol{\beta}}{d\eta}\right]^2\right\}. \tag{15}$$

To compute loss rates using Eqs. (14) and (15) we need to borrow a few more equations from Ref. [20], namely,

$$\beta_x(\eta)=\frac{1}{\gamma(\eta)}\left[qf(\eta)-\frac{\omega_c}{c}y(\eta)\right], \tag{16}$$

$$\beta_y(\eta)=\frac{1}{\gamma(\eta)}\left[\frac{\omega_c}{c}x(\eta)\right], \tag{17}$$

$$\beta_z(\eta)=1-\frac{\gamma_0}{\gamma(\eta)}(1-\beta_0), \tag{18}$$

where $f(\eta)=\sin^2(\kappa\eta/2)\cos\eta$ used to model the laser pulse in Eq. (2). Equations (16)–(18) give the components of the electron velocity vector scaled by the speed of light in

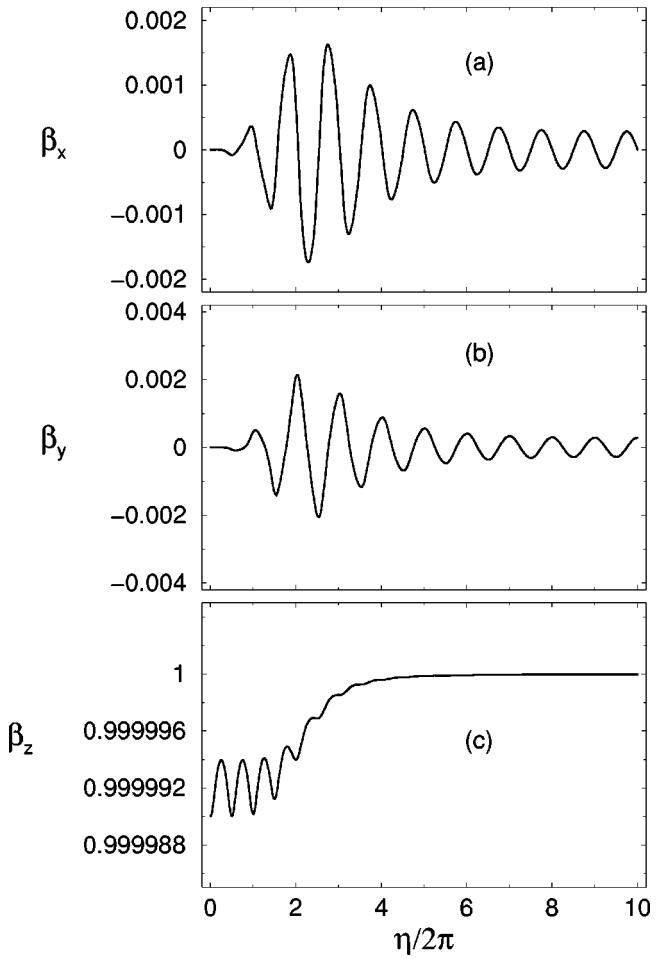

FIG. 5. Velocity components, scaled by the speed of light in vacuum, of the electron whose trajectory is given in Fig. 2, vs the number of field cycles in the pulse.

vacuum. These velocity components are shown vs the number of field cycles in Fig. 5 for $q=1$ and $B_s=30$ T. Note that the three components exhibit oscillations during interaction with the first few field cycles, but soon afterward β_z grows and β_x and β_y decline in absolute value.

Next we calculate the loss rate using Eqs. (14)–(18). The results for a number of cases are presented graphically. Figure 6 shows how the ratio Γ varies during 10 laser cycles and in Fig. 7 we show the energy gain as a function of the interaction time. [Recall that $t=\eta/\omega_l+z(\eta)/c$.] Figure 7(a) was calculated for the field intensity corresponding to $q=1$ and Fig. 7(b), for $q=100$. It is interesting to note that although the pulse employed has a duration of $\tau\approx 13$ fs, nevertheless the motion of the electron is shown over a much longer interaction time [roughly 260 ns in Fig. 7(a) and about 2.6 ms in Fig. 7(b)]. In other words, due to the high speed with which it moves during the interaction time, the electron *rides* with the pulse for a time much longer than the pulse's duration. It is quite evident from both figures that radiation losses are negligibly small by comparison to the rate at which the electron gains energy from the field.

Another feature of the exchange of energy, more evident in Fig. 6(a) than in Fig. 6(b), is that the loss rate reaches a

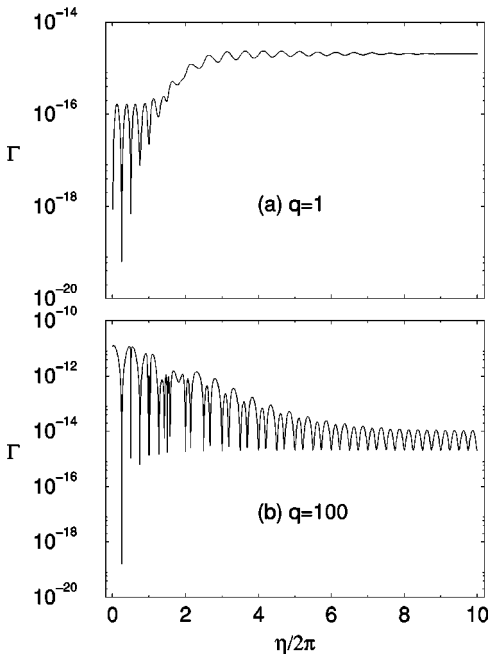

FIG. 6. Ratio of the radiated energy to the energy gain per laser oscillation vs the number of field cycles.

steady maximum value toward the end of the interaction period. This explains the saturation exhibited by the curve of energy gain vs time of Fig. 7, during the same time interval.

V. EMISSION SPECTRA

We have seen in Sec. IV that under the cyclotron resonance condition, a small part of the energy absorbed by the electron from the laser field is reemitted. It is well known that a particle moving at relativistic speeds emits radiation

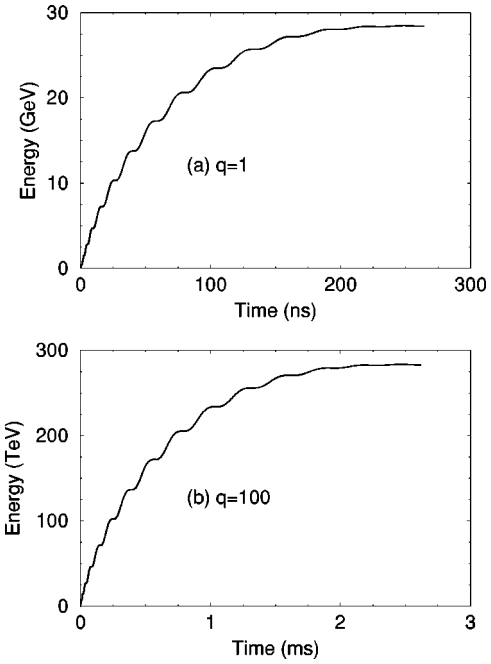

FIG. 7. Evolution in time of the electron energy.

mostly in a small cone around its instantaneous direction of motion. In addition, the emitted radiation has a frequency distribution. Because of current interest in the generation of harmonics of the radiation field, we study the emission spectra in this section. We will investigate both the forward and the backscattered spectra as well as those emitted in the directions of the electric and magnetic field components of the laser field.

The spectra are calculated using the same procedure as in [19,20] starting with the well-known expression of radiant energy emitted per unit solid angle $d\Omega$ and per unit frequency interval $d\omega$ [21],

$$\frac{d^2E(\omega,\Omega)}{d\Omega\, d\omega}=\frac{e^2}{4\pi^2 c}\left|\int_0^T \frac{\mathbf{n}\times[[\mathbf{n}-\boldsymbol{\beta}(t)]\times\dot{\boldsymbol{\beta}}(t)]}{[1-\mathbf{n}\cdot\boldsymbol{\beta}(t)]^2}\times\exp\left\{i\omega\left[t-\frac{\mathbf{n}\cdot\mathbf{r}(t)}{c}\right]\right\}dt\right|^2. \tag{19}$$

In this equation E is used to denote the radiated energy, $\mathbf{n}$ is a unit vector in the direction of propagation of the emitted radiation (direction of observation), $\dot{\boldsymbol{\beta}}=d\boldsymbol{\beta}/dt$, and T is the time interval over which the incident field *seen by the electron* is nonzero. In order to make Eq. (19) easy to program, a change of integration variable is made from t to η with the help of the chain rule of differentiation together with Eq. (10).

A typical generated frequency spectrum is given by the *doubly differential emission cross section*. This quantity may be obtained by dividing the radiant energy, emitted into a unit solid angle per unit frequency per unit time, by the incident energy flux, $(eq\omega_0)^2/8\pi c r_0^2$, r_0 being the classical electron radius. Thus

$$\frac{d^2\sigma(\omega,\Omega)}{d\Omega\, d\omega}=\frac{1}{T}\frac{8\pi c r_0^2}{(eq\omega_l)^2}\frac{d^2E(\omega,\Omega)}{d\Omega\, d\omega}. \tag{20}$$

The doubly differential cross sections are calculated on the basis of Eqs. (19) and (20) and are plotted below against the scattered frequency, with the latter expressed in units of the laser frequency ω_l. Atomic units, with $e=m=1$, will be used. In Fig. 8 we show the forward and backscattered spectra over one decade of laser frequencies. The forward spectrum has one peak corresponding to the laser fundamental (pump) frequency. We have shown previously [20] that the forward spectrum has another peak at $\omega/\omega_l=r$, but due to the resonance condition this peak coincides with the fundamental peak here. Furthermore, for the value of $\kappa=0.1$ used here, the two sidebands discussed in Ref. [20] are also engulfed by the fundamental (Thomson) peak. In a recent article, we have also shown [22] analytically that the spectrum of the backscattered radiation consists of very many peaks spaced closely on the frequency scale in contradistinction to the usual harmonic spectra. We note that an anharmonic frequency distribution has been found by Hartemann *et al.* [23] in the absence of the uniform magnetic field as well.

Very rich (but less accurate) spectra are also shown in Figs. 9 and 10 for observation along the direction of laser

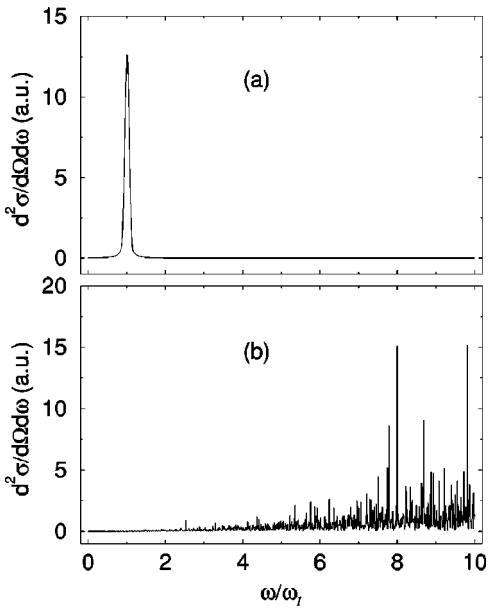

FIG. 8. Forward (top) and backscattered (bottom) spectra. The electron is assumed to have been injected initially, with energy that satisfies the resonance condition, along the propagation direction of a laser pulse of peak intensity corresponding to $q=0.01$ and having 10 field cycles and a wavelength $\lambda=800$ nm. The uniform magnetic field has strength $B_s=30$ T. For this magnetic field strength and laser wavelength, the resonance condition is met for an injection energy of about 114 MeV.

polarization and in the direction of the magnetic component of the laser field. We are still hesitant to interpret these spectra pending a more accurate numerical calculation [24]. Suffice it to say here perhaps that the spectrum along the polarization direction, Fig. 9(a), appears to be richer than that along the laser magnetic field direction, Fig. 9(b), as ex-

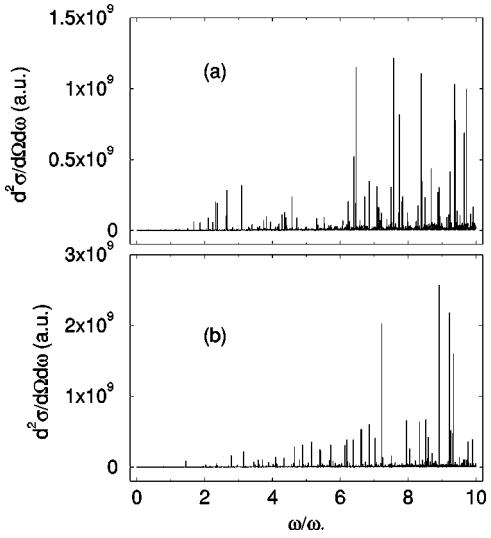

FIG. 9. (a) Spectrum emitted along the electric component of the laser field. (b) Spectrum emitted along the magnetic component of the laser field. The laser field intensity corresponds to $q=1$, and the other electron and field parameters are the same as those of Fig. 8.

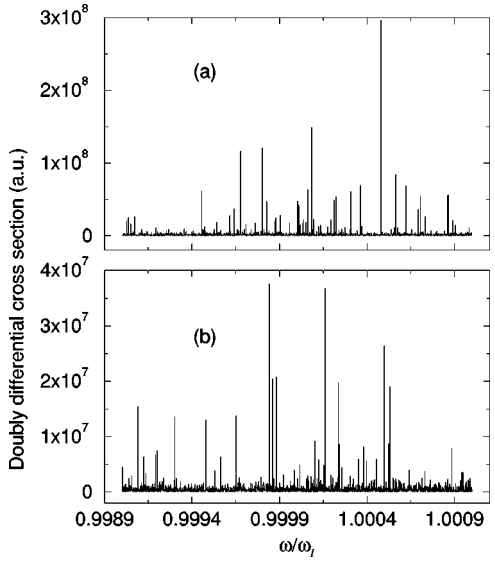

FIG. 10. (a) Spectrum emitted along the electric component of the laser field over a small frequency interval for an off-resonance scenario with $\gamma_0=200$. (b) The corresponding spectrum when the condition for resonance is fulfilled, $\gamma_0\approx 223.594$. The laser field intensity corresponds to $q=1$, and the other electron and field parameters are the same as those of Fig. 8.

pected. Furthermore, a simple formula predicting the frequencies that would be observed along an arbitrary angle to the laser propagation direction has been reported by us recently [19] for the general off-resonance conditions. When the said formula is adapted to suit the condition of resonance $(r=1)$ and after the appropriate observation angle is selected, it still predicts the existence of a tremendous number of closely spaced emission frequencies.

Finally, in Fig. 10 we illustrate the difference between an off-resonance spectrum and an on-resonance one. To this end a small portion of the spectrum shown in Fig. 9(a) around $\omega=\omega_l$ has been calculated under both conditions and is shown in Fig. 10. Figure 10(a) corresponds to $\gamma_0=200$, i.e., one that does not meet the resonance condition, while Fig. 10(b) is for $\gamma_0=223.594$, i.e., for almost exact resonance. We notice a substantial reduction in the strength of the lines in going from Figs. 10(a) and 10(b). This demonstrates quite clearly the resonance absorption of energy by the electron from the radiation field. Given the fact that these spectra are not highly accurate, it is almost impossible to draw conclusions about the number of emission lines in each.

VI. CONCLUSIONS

We have studied in detail a scheme, dependent upon an initial resonance condition between the Doppler-shifted laser frequency and the cyclotron frequency, for accelerating an electron in vacuum to extremely high energies by an intense $\sin^2$ laser pulse and in the presence of a strong uniform magnetic field. For the field parameters $\lambda=800$ nm and $B_s=30$ T (chosen for the sake of concreteness in the illustrations) one finds that the resonance may be achieved in practice for an initial electron injection energy of about 114 MeV. This can be ensured by preacceleration to that energy before the electron is subjected to the laser and magnetic field environment for further acceleration. It has been shown that an acceleration gradient in the GeV/m range can be achieved for interaction with a pulse of several cycles that also leads to a rather large longitudinal travel distance of the electron. More significantly, it has been shown that acceleration gradients of many TeV/m can be achieved if the electrons are extracted from the interaction region after encountering the first *quarter cycle* of the laser pulse. In this case the electron can be accelerated to very high energies within a drastically reduced longitudinal travel distance. This, however, requires the use of very high laser field intensities.

We also show that the radiation losses that accompany the above acceleration process remain small. The relatively weak associated emission spectra are found to depend strongly on the direction of emission and are in general composed of irregular distributions of emission lines. More concrete conclusions concerning the emission spectra should perhaps await a more accurate calculation than has been done here.

ACKNOWLEDGMENTS

Y.I.S. acknowledges, with thanks, financial support for this work from the Alexander von Humboldt Stiftung in Bonn, Germany. He also thanks the Fakultät für Physik at Universität Bielefeld and the Fakultät für Physik at Universität Freiburg for hospitality during part of the time this work was carried out. This work was partially supported by DFG, Bonn, under the SPP ''Relativistische Effekte.''

[1] C.R. Menyuk, A.T. Drobot, K. Papadopoulos, and H. Karimabadi, Phys. Rev. Lett. **58**, 2071 (1987).
[2] C.E. Clayton, K.A. Marsh, A. Dyson, M. Everett, A. Lal, W.P. Leemans, R. Williams, and C. Joshi, Phys. Rev. Lett. **70**, 37 (1993).
[3] A.A. Chernikov, G. Schmidt, and A.I. Neishtadt, Phys. Rev. Lett. **68**, 1507 (1992).
[4] M.S. Hussein, M.P. Pato, and A.K. Kerman, Phys. Rev. A **46**, 3562 (1992).
[5] W.D. Kimura *et al.*, Phys. Rev. Lett. **74**, 546 (1995).
[6] A. van Steenbergen *et al.*, Phys. Rev. Lett. **77**, 2690 (1996).
[7] E. Esarey *et al.*, IEEE Trans. Plasma Sci. **24**, 252 (1996).
[8] K. Nakajima *et al.*, Phys. Rev. Lett. **74**, 4428 (1995).
[9] E. Esarey, B. Hafizi, R. Hubbard, and A. Ting, Phys. Rev. Lett. **80**, 5552 (1998).
[10] A. Ting *et al.*, Phys. Plasmas **4**, 1889 (1997).
[11] C.I. Moore *et al.*, Phys. Rev. Lett. **79**, 3909 (1997).
[12] D. Gordon *et al.*, Phys. Rev. Lett. **80**, 2133 (1998).
[13] J.X. Wang, Y.K. Ho, Q. Kong, L.J. Zhu, L. Feng, S. Scheid, and H. Hora, Phys. Rev. E **58**, 6575 (1998).
[14] T. Häuser, W. Scheid, and H. Hora, Phys. Lett. A **186**, 189 (1994).
[15] C.S. Roberts and S.J. Buchsbaum, Phys. Rev. **135**, A381 (1964).
[16] A. Loeb and L. Friedland, Phys. Rev. A **33**, 1828 (1986).
[17] A. Loeb and S. Eliezer, Phys. Rev. Lett. **56**, 2252 (1986).

[18] A. Loeb, L. Friedland, and S. Eliezer, Phys. Rev. A **35**, 1692 (1987).
[19] Y.I. Salamin and F.H.M. Faisal, Phys. Rev. A **58**, 3221 (1998).
[20] F.H.M. Faisal and Y.I. Salamin, Phys. Rev. A **60**, 2505 (1999).
[21] J.D. Jackson, *Classical Electrodynamics*, 2nd ed. (Wiley, New York, 1975).
[22] Y.I. Salamin, Phys. Rev. A **60**, 3276 (1999).
[23] F.V. Hartemann, A.L. Troha, and N.C. Luhmann, Phys. Rev. E **54**, 2956 (1996).
[24] Y.I. Salamin *et al.* (unpublished).